Fiber Length and Orientation in Long-Fiber Injection-Molded Thermoplastics – Part I: Modeling of Microstructure and Elastic Properties*

BA NGHIEP NGUYEN,† SATISH K. BAPANAPALLI,
JAMES D. HOLBERY AND MARK T. SMITH
Pacific Northwest National Laboratory, P.O. Box 999, Richland, WA 99352, USA

VLASTIMIL KUNC AND BARBARA J. FRAME
Oak Ridge National Laboratory, P.O. Box 2009, Oak Ridge, TN 37831, USA

JAY H. PHELPS AND CHARLES L. TUCKER III
University of Illinois at Urbana-Champaign, Department of Mechanical Science and Engineering, Urbana, IL 61801, USA

ABSTRACT: This article develops a methodology to predict the elastic properties of long-fiber injection-molded thermoplastics (LFTs). The corrected experimental fiber length distribution and the predicted and experimental orientation distributions were used in modeling to compute the elastic properties of the composite. First, from the fiber length distribution (FLD) data in terms of number of fibers versus fiber length, the probability density functions were built and used in the computation. The two-parameter Weibull's distribution was also used to represent the actual FLD. Next, the Mori–Tanaka model that employs the Eshelby's equivalent inclusion method was applied to calculate the stiffness matrix of the aligned fiber composite containing the established FLD. The stiffness of the actual as-formed composite was then determined from the stiffness of the computed aligned fiber composite that was averaged over all possible orientations using the orientation averaging method. The methodology to predict the elastic properties of LFTs was validated via experimental verification of the longitudinal and transverse moduli determined for long glass fiber injection-molded polypropylene specimens. Finally, a sensitivity analysis was conducted to determine the effect of a variation of FLD on the composite elastic properties. Our analysis shows that it is essential to obtain an accurate fiber

*This manuscript has been authored by Battelle Memorial Institute, Pacific Northwest Division, under Contract No. DE-AC06-76RL0 1830 with the U.S. Department of Energy. The United States Government retains and the publisher, by accepting the article for publication, acknowledges that the United States Government retains a non-exclusive, paid-up, irrevocable, world-wide license to publish or reproduce the published form of this manuscript, or allow others to do so, for United States Government purposes.
†Author to whom correspondence should be addressed. E-mail: ba.nguyen@pnl.gov
Figure 3 appears in color online: http://jcm.sagepub.com

0021-9983/08/10 1003–27 $10.00/0 DOI: 10.1177/0021998308088606
© SAGE Publications 2008
Los Angeles, London, New Delhi and Singapore

Downloaded from jcm.sagepub.com at OAK RIDGE NATIONAL LABORATORY on December 1, 2015

orientation distribution and a realistic fiber length distribution to accurately predict the composite properties.

KEY WORDS: long-fiber thermoplastics, injection molding, fiber length distribution, fiber orientation, elastic properties.

INTRODUCTION

LONG-FIBER REINFORCED THERMOPLASTICS (LFTs) have generated great interest within the automotive industry. These materials that have already been used for semi-structural applications are now candidate materials for structural applications to reduce vehicle weight. LFTs produced by injection-molding present the advantage of low cost part production since conventional injection-molding equipment can be adjusted with some specific tool design to produce LFT parts. It is well known that LFTs offer much better mechanical performance than the short-fiber counterparts since the use of long fibers leading to higher fiber aspect ratios considerably increases the composite stiffness and strength, and enhances creep and fatigue endurance [1,2]. Although LFTs have been commercially available for mostly twenty years and have been used in the automotive industry for more than fifteen years [3], there exists little experimental and modeling work on these materials.

In order for LFTs to be used efficiently and safely for structural applications, it is essential to be able to (i) predict their microstructure as a function of the constituents' properties and characteristics as well as processing parameters, (ii) predict their thermoelastic properties and nonlinear responses as a function of the as-formed microstructure, and (iii) establish reliable characterization methods for obtaining all the necessary microstructural features for the model validation. While this paper partly addresses point (ii) that focuses on the prediction of the elastic properties for a studied LFT system produced by injection molding, it also addresses point (i) by comparing current fiber orientation models to experiments, and assessing their usefulness for modeling LFTs. The property prediction for LFTs requires the knowledge of two essential microstructural features in addition to the constituents' material properties: fiber orientation distribution (FOD) and fiber length distribution (FLD). In this article, the FODs for the long fiber glass/polypropylene (PP) injection-molded center-gated disk and ISO-plaque were first experimentally determined using the method developed in Ref. [4]. Next, the FOD predictions in these samples were achieved using ORIENT, a finite difference code developed at the University of Illinois. A method for the measurement of FLDs was developed to obtain the FLD for the same samples. The details of the FLD measurement method will be described in our forthcoming paper that focuses on the experimental and characterization aspects [5]. Significant fiber breakage has occurred during injection molding as observed through our fiber length measurement. This phenomenon was previously discussed in for example, Refs [6] and [7] for various short- and long-fiber thermoplastics.

The current approach to predict the elastic properties of a discontinuous fiber composite includes two key steps. The first step is to compute the elastic stiffness of a 'reference' composite that contains unidirectional fibers having the same features, volume fraction and length distribution as for the actual composite. Second, the stiffness of the actual as-formed composite is obtained from the stiffness of the reference composite that is averaged over all possible orientations using the orientation averaging technique [8,9].

Downloaded from jcm.sagepub.com at OAK RIDGE NATIONAL LABORATORY on December 1, 2015

There is a large body of literature addressing the computation of the elastic stiffness for the aligned fiber composite using micromechanical modeling or numerical simulations of a composite representative volume element. To date, the Eshelby's equivalent inclusion method [10] combined with the Mori–Tanaka model [11] (termed as the Eshelby–Mori–Tanaka model) are one of the most effective models in terms of accuracy and efficiency of the prediction [12]. Tucker and Liang [13] have conducted a review and evaluation of standard micromechanical models for predicting elastic properties of short-fiber composites. These authors have shown that the Eshelby–Mori–Tanaka (EMT) model provides accurate predictions of their finite element results and have recommended this model as the best choice for estimating the stiffness of aligned short-fiber composites. More recently, Hine et al. [14] have used the Monte-Carlo technique to generate randomly non-overlapping aligned fiber microstructures containing a distribution of fiber lengths. These authors have then carried out a numerical simulation of the generated microstructure and have shown that their simulation results agreed well with the Tandon–Weng model's prediction. The Tandon–Weng model [15] is identical to the EMT model. Later, Hine et al. have applied the same method to generate randomly oriented fiber microstructure [16] and have demonstrated that the elastic and thermoelastic properties obtained by numerical simulations are very close to the results determined by the constant strain orientation averaging method (averaging the stiffness constants) [8,9]. Hine et al. [16] also recommended an EMT type model (e.g., the Tandon–Weng model) combined with the orientation averaging approach to compute the elastic and thermoelastic properties of short-fiber composites.

In view of all the previous studies, this paper applies an EMT type model and the orientation averaging method proposed in Refs [8] and [9] to compute the elastic stiffness for a LFT composite system. The EMT formulation proposed in Ref. [17] and also used in Ref. [18] is employed in the present article. The experimental FLD data was corrected by a method proposed in Ref. [19] and was then expressed for weight of fibers to be used in the computation of the stiffness of the reference aligned fiber composite. A two-parameter Weibull's distribution was also employed to fit the corrected FLD. In addition, the measured and predicted FODs through the specimen thickness were utilized in the orientation averaging procedure to compute the stiffness of the as-formed composite along the thickness direction. Assessment of fiber orientation modeling was carried out to determine improvements needed for more accurate predictions. Finally, the effect of FLD on the resulting elastic properties was also investigated in a sensitivity analysis to determine how accurate the measured FLD should be for acceptable property predictions.

THEORY

Description of Fiber Length

A common description of the length distribution is the probability density function $f(l)$ defined such that the probability of a fiber having a length between l and $l + \mathrm{d}l$ is $f(l)\,\mathrm{d}l$. This function must be normalized such that

$$\int_0^\infty f(l)\,\mathrm{d}l = 1. \tag{1}$$

Downloaded from jcm.sagepub.com at OAK RIDGE NATIONAL LABORATORY on December 1, 2015

From this function the properties such as the number-average length $\bar{L}_{\mathrm{n}}$, and the weight-average length $\bar{L}_{\mathrm{n}}$, can be calculated:

$$\bar{L}_{\mathrm{n}} = \int_0^\infty f(l)l\,\mathrm{d}l \tag{2}$$

$$\bar{L}_{\mathrm{w}} = \frac{\int_0^\infty f(l)l^2\,\mathrm{d}l}{\int_0^\infty f(l)l\,\mathrm{d}l}. \tag{3}$$

From the raw FLD data, the discrete approximation of $f(l_i)$ is $\tilde{f}_i$ given by:

$$\tilde{f}_i = \frac{N_i}{\Delta l \sum_i N_i} \tag{4}$$

where Δl is the experimental bin width, and a set of length values (bin centers) l_i such that $l_{i+1} = l_i + \Delta l$. The lengths l_i span the range of the data. N_i is the number of fibers with lengths between $l_i - \Delta l/2$ and $l_i + \Delta l/2$. Equation (2) can be approximated as:

$$\bar{L}_{\mathrm{n}} = \sum_i \tilde{f}_i l_i \Delta l = \frac{\sum_i N_i l_i}{\sum_i N_i}. \tag{5}$$

An alternate FLD representation is a probability density function for weight, $w(l)$ [20] that is related to $f(l)$ as:

$$w(l) = \frac{f(l)l}{\int_0^\infty f(l)l\,\mathrm{d}l} = \frac{f(l)l}{\bar{L}_{\mathrm{n}}}. \tag{6}$$

As $f(l)$, $w(l)$ must be normalized:

$$\int_0^\infty w(l)\,\mathrm{d}l = 1. \tag{7}$$

Similar to Equation (4), the discrete approximation to $w(l_i)$ using the experimental/histogram data is:

$$\tilde{w}_i = \frac{N_i l_i}{\Delta l \sum N_i l_i}. \tag{8}$$

Also, the weight-average length can be approximated as:

$$\bar{L}_{\mathrm{w}} = \frac{\sum N_i l_i^2}{\sum N_i l_i}. \tag{9}$$

The maximum entropy approach can be used to assign a probability density function to a measured fiber length distribution. The principle of this approach is that among all probability density functions that are consistent with the specified information, the

Downloaded from jcm.sagepub.com at OAK RIDGE NATIONAL LABORATORY on December 1, 2015

probability density function that has maximum information entropy contains no more information than that specified [21].

A Two-Parameter Weibull's Distribution to Fit the Experimental FLD

The measurement of fiber lengths in LFT samples show that the actual fiber length distributions are unsymmetrical and exhibit a shape having a sharp peak in the short fiber range and a long 'tail' towards the long fiber range (>1 mm). There are two suitable distribution functions that can be used to represent an actual FLD: Weibull's and log-normal distribution functions [20]. The two-parameter Weibull's distribution is used in this article in view of its simple and practical form. The shape parameters b and c can take different values to represent various shapes of practical FLDs. The Weibull's probability distribution function is given by:

$$p(l) = \frac{c}{b}\left(\frac{l}{b}\right)^{c-1} e^{-(l/b)^c} \tag{10}$$

where l is the fiber length. The shape parameters b and c are determined by methods based on maximum likelihood technique [22]. The likelihood function for the two-parameter Weibull distribution is given by the following equation:

$$L = \prod_{i=1}^{N_t} \left(\frac{c}{b}\right)\left(\frac{l_i}{b}\right)^{c-1} e^{-(l_i/b)^c} \tag{11}$$

N is the total number of data points used for Weibull fit. The following system of equations is obtained by maximizing the log of the likelihood function:

$$\frac{\sum_{i=1}^{N_t} (l_i)^c \mathrm{In}(l_i)}{\sum_{i=1}^{N} (l_i)^c} - \frac{1}{N_t}\sum_{i=1}^{N_t} \mathrm{In}(l_i) - \frac{1}{c} = 0 \tag{12}$$

and

$$b = \left[\left(\sum_{i=1}^{N_t} (l_i)^c\right)\frac{1}{N_t}\right]^{1/c}. \tag{13}$$

Equation (12) can be solved for c using the Newton–Raphson iterative method, and the value of c is then substituted in Equation (13) to obtain the value of b.

Orientation Tensors

The fiber orientation in a discontinuous fiber composite can be described by the orientation tensors defined by Advani and Tucker [8]. These tensors are theoretically given in terms of the orientation vector that is parallel to the fiber axis. As it is not possible and necessary to quantify the orientation of each fiber in the composite, the fiber orientation is defined over a volume domain, thus it has a volume average sense. Practically, the

Downloaded from jcm.sagepub.com at OAK RIDGE NATIONAL LABORATORY on December 1, 2015

second- and fourth-order orientation tensors are used in the computation. These tensors are defined as:

$$A_{ij} = \langle p_i p_j \rangle \tag{14}$$

$$A_{ijkl} = \langle p_i p_j p_k p_l \rangle \tag{15}$$

where the bracket '$\langle\ \rangle$' denotes the average quantity over a volume domain, p_i are the components of the orientation vector, $\mathbf{p}$. The orientation tensors can be related to the probability distribution function ψ ($\mathbf{p}$) by assuming that all the fibers in the averaging volume are drawn down from a population with the same probability distribution function:

$$A_{ij} = \int \psi(\mathbf{p}) p_i p_j \, \mathrm{d}\mathbf{p} \tag{16}$$

$$A_{ijkl} = \int \psi(\mathbf{p}) p_i p_j p_k p_l \, \mathrm{d}\mathbf{p}. \tag{17}$$

Among the nine components of A_{ij}, only five are independent. Three of the remaining components are determined by symmetry:

$$A_{ij} = A_{ji}. \tag{18}$$

The last component is determined by the fact that $\mathbf{p}$ has a unit length and $p_1 p_1 + p_2 p_2 + p_3 p_3 = 1$ for every fiber so that:

$$A_{11} + A_{22} + A_{33} = 1. \tag{19}$$

Applying similar symmetry conditions to the fourth-order tensor A_{ijkl} shows that it has fourteen independent components. The fourth-order tensor also contains all the information in the second-order tensor because $A_{ij} = A_{ijkk}$. The A_{ij} components can be measured and predicted, but a closure approximation is necessary to estimate the components of the fourth-order tensor A_{ijkl} in terms of A_{ij}. There exists a significant body of literature on closure approximations, for example Refs [7] and [23], and to date the ORE orthotropic closure approximation [24] is the most accurate one and has been used in this article.

Prediction of Fiber Orientation Distribution

In order to compute the orientation state for an injection molding operation, the equations of balance of mass, momentum, and energy must be solved so that a velocity field can be computed. A program named ORIENT developed by the University of Illinois was used in this article to solve for the velocity profile and the orientation in the center-gated disk and ISO-plaque geometries [25]. ORIENT is a finite difference program that was designed to calculate the velocity field and second-order orientation tensor during mold filling for these geometries. ORIENT also takes into account non-isothermal conditions and solves for the temperature field within the mold. It uses the Hele–Shaw approximation [26] and the decoupled flow/orientation approach where the velocity

Downloaded from jcm.sagepub.com at OAK RIDGE NATIONAL LABORATORY on December 1, 2015

solution is decoupled from the orientation solution. The flow-induced fiber orientation is depicted by the reduced strain closure (RSC) model described in Ref. [27]:

$$\frac{DA_{ij}}{D_t} = \frac{1}{2}\left(A_{ik}\omega_{kj} - \omega_{ik}A_{kj}\right) + \frac{\kappa}{2}\left(A_{ik}\dot{\gamma}_{kj} + \dot{\gamma}_{ik}A_{kj} - 2\left[A_{ijkl} + \left(1 - \frac{1}{SRF}\right)\left(L_{ijkl} - M_{ijmn}A_{mnkl}\right)\right]\dot{\gamma}_{kl}\right) + \frac{2C_I\dot{\gamma}}{SRF}\left(\delta_{ij} - 3A_{ij}\right) \tag{20}$$

where ω_{ij} is the vorticity tensor, and $\dot{\gamma}_{ij}$ is the rate of the deformation tensor whose scalar magnitude is $\dot{\gamma}$. δ_{ij} is the identity tensor. κ and C_{I} are material constants; κ depends on the fiber aspect ratio and for long rigid cylinders is approximately equal to $\kappa = ((l/d)^2 - 1/(l/d)^2 + 1)$. In case of slender particles (e.g., long fibers), κ approaches unity, and the presence of the interaction term inhibits fiber tumbling; hence the fiber length does not affect fiber orientation through this parameter, and we use $\kappa = 1$. C_{I} is called the fiber–fiber interaction coefficient, and SRF is an empirical parameter termed as strain reduction factor that is introduced to reduce the rate of fiber alignment in concentrated fiber suspensions. If $SRF = 1$, the Folgar–Tucker [8,28] model is recovered. In practice, coefficients C_{I} and SRF are identified by fitting the predicted result for A_{11} to the measured value for this component. The ORE closure approximation [23,24] is used to estimate the fourth-order tensor A_{ijkl} from A_{ij}. L_{ijkl} and M_{ijkl} are fourth-order tensors formed from the eigenvalues and eigenvectors of A_{ij} [27].

It is important to emphasize that Equation (20) was established for short-fiber systems and has been a first step to improve the Folgar–Tucker model in order to predict fiber orientation in concentrated suspensions. The short-fiber range is related to fiber lengths that are much less than 1 mm. Equation (20) does not capture the effect of fiber length distribution on fiber orientation. Fiber orientation prediction shows that values of C_{I} for LFTs are much larger than those for SFTs and the effect of choosing $SRF > 1$ is to widen the core of an LFT skin/shell/core fiber orientation layer structure. Increasing C_{I} will decrease the alignment in the flow direction but increase the alignment the cross-flow and thickness directions. It has been observed that the LFT core is significantly larger than that of a short-fiber thermoplastic composite [29]. To date no models have been established for predicting fiber orientation due to the flow of a long-fiber suspension. One of the goals of our work is to assess the applicability of Equation (20) when it is applied to predict long-fiber orientation. This assessment will allow us to determine the limitations of the current fiber orientation model in order to develop a new model for LFTs. Another important issue that needs to be mentioned is the wall effect. It is always possible that wall effects are important. It is equally possible that the fiber–fiber interactions are so strong in LFTs that the wall effect would not be important.

Prediction of Elastic Properties

The stiffness matrix of a unidirectional (UD) fiber composite containing a fiber length distribution is given by:

$$C_{ijkl} = \frac{\int_0^\infty C^*_{ijkl}(l/d)p(l)\,\mathrm{d}l}{\int_0^\infty p(l)\,\mathrm{d}l} \tag{21}$$

Downloaded from jcm.sagepub.com at OAK RIDGE NATIONAL LABORATORY on December 1, 2015

where $C^*_{ijkl}(l/d)$ is the stiffness matrix of the UD fiber composite having the aspect ratio l/d. $p(l)$ is the probability density function that can be expressed for number or weight of fibers. In this paper $p(l)$ for weight of fiber lengths ($p(l) = w(l)$) is used in the calculation of the composite elastic properties. From a theoretical viewpoint one can argue for using the weight distribution of length $w(l)$ rather than the number distribution $f(l)$ since the process of averaging over the length distribution is essentially a volume average, and $w(l)$ is proportional to the volume of fibers of length l. The Eshelby–Mori–Tanaka (EMT) method developed in Refs [17] and 18] was applied to compute $C^*_{ijkl}(l/d)$, and after the calculation of the resulting C_{ijkl} using Equation (21), the elastic stiffness of the actual composite having an as-formed fiber orientation state was computed using the orientation averaging method [8,9]:

$$\begin{aligned}\bar{C}_{ijkl} = {} & B_1 A_{ijkl} + B_2\left(A_{ij}\delta_{kl} + A_{kl}\delta_{ij}\right) + B_3\left(A_{ik}\delta_{jl} + A_{il}\delta_{jk} + A_{jl}\delta_{ik} + A_{jk}\delta_{il}\right) \\ & + B_4\delta_{ij}\delta_{kl} + B_5\left(\delta_{ik}\delta_{jl} + \delta_{il}\delta_{jk}\right)\end{aligned} \tag{22}$$

where the coefficients B_i ($i = 1, 5$) are the invariants of the stiffness tensor of the UD transversely isotropic composite (Equation (21)). These coefficients are given in Refs [8] and [9].

The overall stiffness of the composite specimen can be determined by considering the specimen as being formed by a stacking sequence of composite layers having the same thickness. Each layer is characterized by an orientation state. As the stiffness of each layer (that depends on local fiber orientation) has already been computed using Equation (22), the lamination theory can therefore be applied to calculate the overall stiffness of the composite formed by this stacking sequence.

EXPERIMENTAL METHODS AND MATERIALS

Materials and Molding Conditions

Long glass fiber/polypropylene compounds were procured from Montsinger Technologies. The molding compound had a fiber weight fraction of 40%, a nominal fiber length of 13 mm, and a nominal fiber diameter of 17.4 microns. Injection-molding was carried out for the center-gated disk and ISO-plaque geometries. The pellets were injected using two different volume flow rates (16.4 and 131.1 cm^3/s) in order to study the effect of the injection speed on the as-formed composite microstructure. The density of glass/polypropylene measured at the melting state is 1.2203 g/cm^3. In this article, a center-gated disk formed under slow fill conditions (16.4 cm^3/s) and an ISO-plaque formed under fast fill conditions (131.1 cm^3/s) are analyzed. The weight fraction of glass fibers for both geometries is 40%, this leads to 19.2% fiber volume fraction. The center-gated disk is 3 mm thick and has a diameter of 177.8 mm. The ISO-plaque is also 3 mm thick, and is 90 mm long and 80 mm wide. Figures 1 and 2 present the pictures of these injection-molded samples. The gate is a flash gate with a U-shaped runner. The runner is 90 mm long along the edge of the ISO-plaque, 6.35 mm wide and 6.35 mm deep. The thin land or flash between the runner and the part is 1.524 mm thick. The runner was fed through a tapered sprue which is 76.2 mm long and has a starting diameter of 5.461 mm and ending diameter of 8.28 mm. No runner was used for the center-gated disk.

Downloaded from jcm.sagepub.com at OAK RIDGE NATIONAL LABORATORY on December 1, 2015

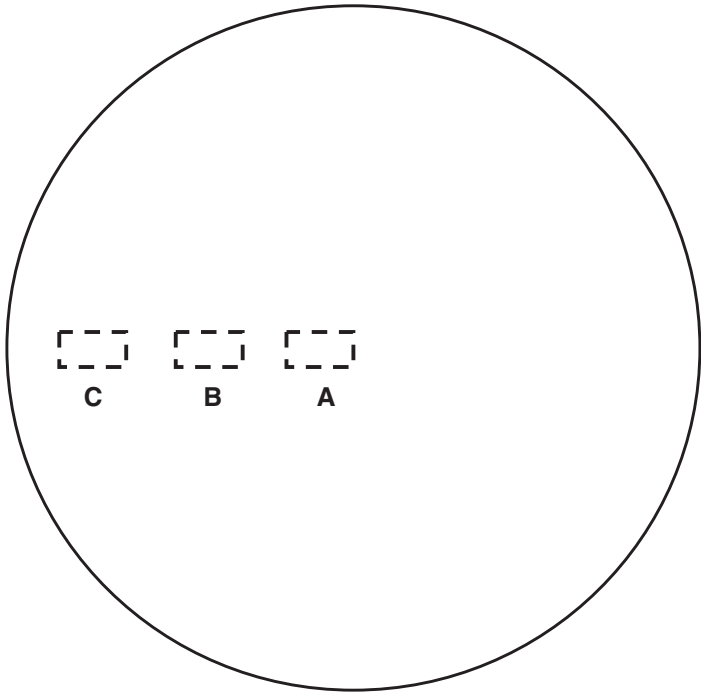

Figure 1. *The 3 mm thick injection-molded glass/PP center-gated disk: Regions A, B, and C being 25.4 mm long along a radial direction were taken for FLD measurement.*

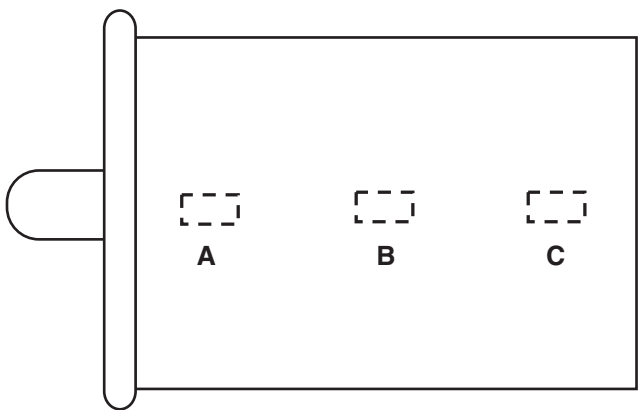

Figure 2. *The 3 mm thick injection-molded ISO-plaque: Regions A, B, and C being 25.4 mm long were taken for FLD measurement.*

Fiber Length and Orientation Measurements

Three regions denoted as A, B, and C located at 6, 34, and 64 mm on the center-gated disk, and at 15, 45, and 75 mm on the ISO-plaque, respectively, were considered for fiber

Downloaded from jcm.sagepub.com at OAK RIDGE NATIONAL LABORATORY on December 1, 2015

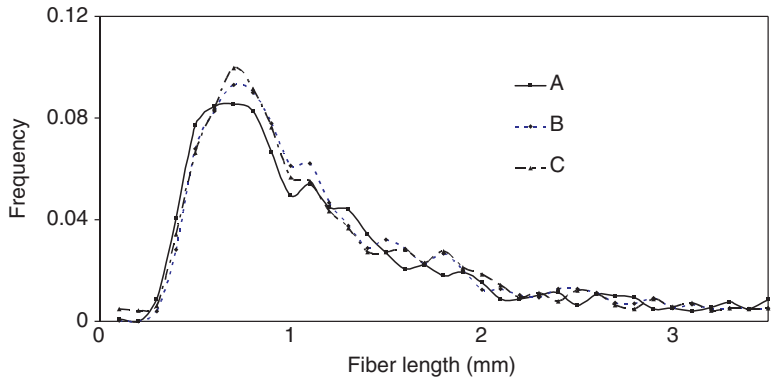

Figure 3. *Fiber length distributions in terms of frequency vs fiber length at the regions A, B, and C of the glass/PP center-gated disk.*

length and orientation measurements. A population of 2000 fibers was taken in each region for fiber length measurement. The FLD measurement method will be described in our forthcoming article [5] and is summarized as follows. The matrix of a relatively large sample is burned off, and a mat of fibers remains. A small amount of epoxy resin is deposited through the thickness of this fiber mat and cured, capturing all the fibers that pass through this region. The volume that is encapsulated by the epoxy is called the sampling region. The fibers that do not pass through the sampling region are carefully pulled away, leaving only the sampling region and the fibers captured in it. The epoxy is then burned off, the fibers that remain are separated, and their lengths are measured by image analysis. This FLD measurement method offers an objective way to select a reasonable-size and representative sample of fibers. However, the fibers thus selected represent a biased sample of the fibers. Recently, a method has been proposed to correct the raw FLD to obtain an unbiased estimate of the distribution [19]. The details of the FLD correction method will be presented in our forthcoming article (Part II) that describes the experimental characterization of LFT microstructure [5]. Figure 3 shows the FLDs measured at A, B, and C on the center-gated disk. These distributions reveal little additional fiber length attrition along the radial direction during flow of the fiber suspension. This confirms that fiber length attrition occurs essentially before the fibers enter the mold cavity. As a result, only FLDs measured at the location B were used in the computation of the elastic properties of the as-formed composite.

Polished samples were analyzed for fiber orientation using an optical system developed by Hine et al. [4]. In this paper Hine et al.'s method is termed as the 'Leeds system'. This system collects an array of digital images from a cross-section of a sample and performs assembly of these images. Fibers are assumed to be straight cylinders, therefore the cross-sections of fibers in a given plane should be visible as ellipses. The Leeds system distinguishes fibers from matrix through thresholding, and ellipses were fitted to the thresholded image. Fiber orientation was determined based on the ratio and size of minor and major axes of ellipses fitted to the image. Curved fibers have been observed in the tested samples. If the fibers are curved, the data from the Leeds measurement is the segmental orientation distribution, as compared to the end-to-end orientation distribution. However, recent finite element calculations by Bapanapalli and Nguyen [30] suggest that segmental orientation is the appropriate

Downloaded from jcm.sagepub.com at OAK RIDGE NATIONAL LABORATORY on December 1, 2015

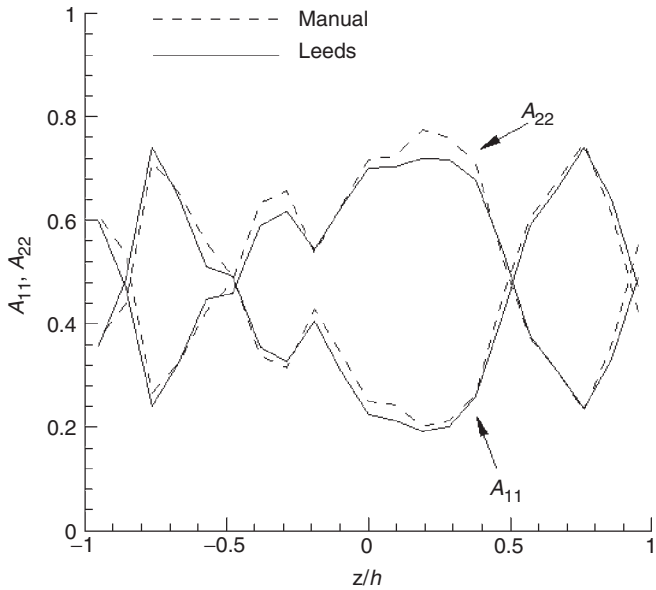

Figure 4. *Fiber orientation results obtained by the Leeds system and manual measurement for region A of a slow-fill glass/PP center-gated disk.*

measure of orientation for micromechanical modeling of gently-curved fibers. To verify the Leeds method's results for LFTs, manual fiber orientation measurement was also performed for the selected regions illustrated in Figures 1 and 2. Figure 4 shows the comparison of through-thickness fiber orientation results obtained by the Leeds method and manual measurement for the region A of a slow-fill glass/PP center-gated disk. On this figure are used the z-coordinates normalized by the specimen thickness, h. Excellent agreement of results has confirmed the validity of the Leeds method for measuring fiber orientation in our LFT samples.

Mechanical Property Measurement

Tensile specimens were cut from the injection-molded samples for mechanical testing. For the ISO-plaque geometry, specimen cutting was carried out along the longitudinal direction to make specimens for obtaining the tensile modulus $\bar{E}_{11}$ while the specimens were cut along the in-plane transverse direction to produce specimens for determining $\bar{E}_{22}$. The specimens that contain the sample edge were excluded from testing due to the edge effect. For the center-gated disk geometry, the specimen cutting was performed along two perpendicular radial directions to obtain $\bar{E}_{11}$ while $\bar{E}_{22}$ was obtained using a specimen that contains the location B in its central region and is perpendicular to the radial direction passing through this location. All specimens are 12.5 mm wide. Servo-hydraulic machine applied tension at constant rate of 0.0254 mm/s. Strain was measured with 12.5 mm gage length extensometer positioned over the area of interest, while stress was calculated from load signal obtained from a load cell and cross-sectional area of the specimen.

Downloaded from jcm.sagepub.com at OAK RIDGE NATIONAL LABORATORY on December 1, 2015

RESULTS AND DISCUSSION

FLD Data and Quality of the Weibull's Fit

Figure 5(a) and (b) show the FLD in terms of probability density functions for weight and numbers determined for region B of the glass/PP ISO-plaque. This figure also presents

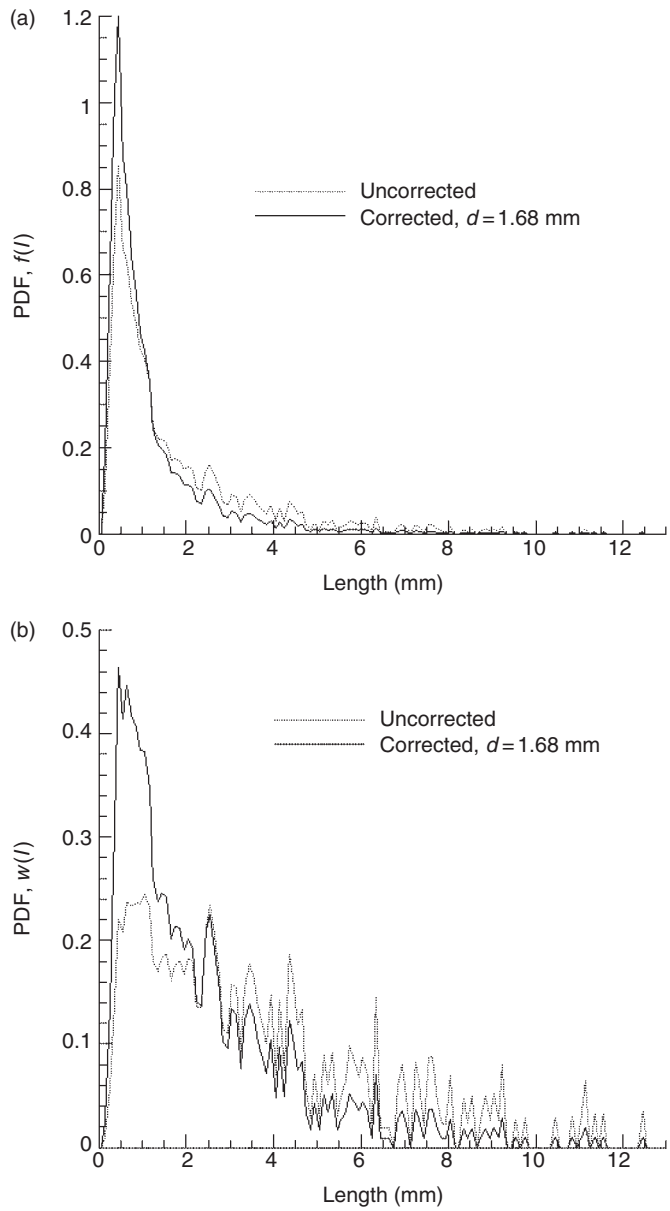

Figure 5. *Probability density functions for (a) number of fibers f(l) and (b) weight of fibers w(l) established from FLD data for the glass/PP ISO-plaque. The corrected distributions are obtained for a sampling region of 1.68 mm diameter.*

Downloaded from jcm.sagepub.com at OAK RIDGE NATIONAL LABORATORY on December 1, 2015

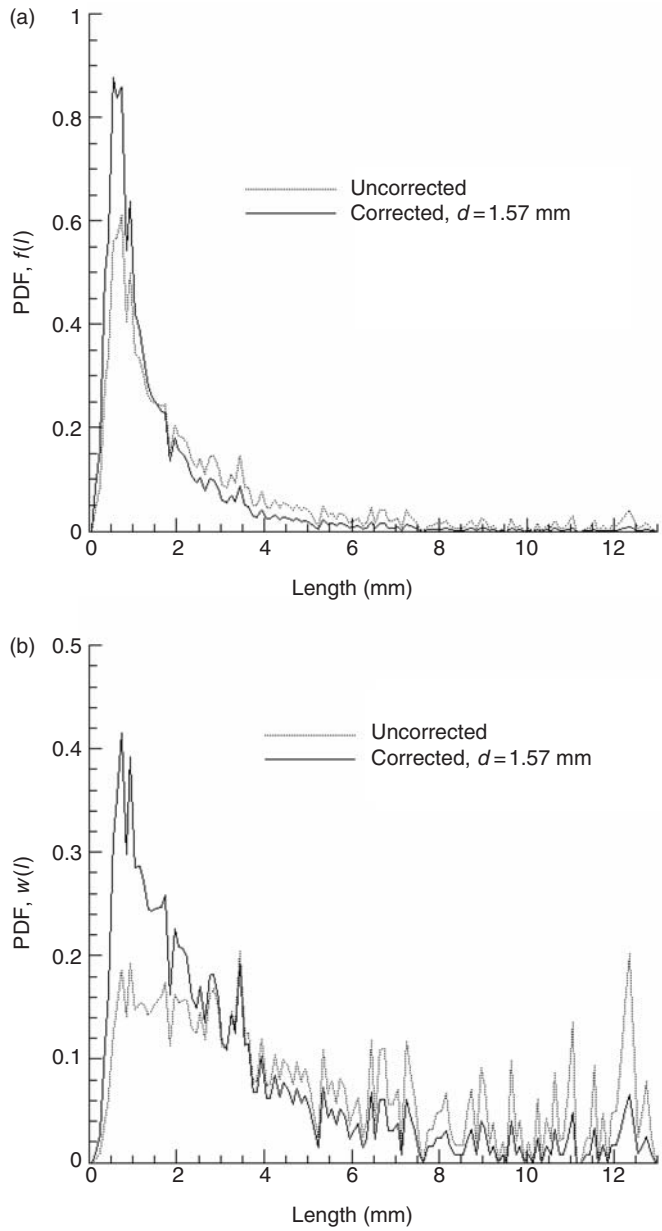

Figure 6. *Probability density functions for (a) number of fibers f(l), and (b) weight of fibers w(l) established from FLD data for the glass/PP center-gated disk. The corrected distributions are obtained for a sampling region of 1.57 mm diameter.*

the FLD corrected using the method presented in Refs [5] and [19] with $d = 1.68$ mm, the measured diameter of the sampling region. The FLD results for region B of the center-gated disk are presented in Figure 6(a) and (b) with $d = 1.57$ mm.

Figure 7(a) shows the Weibull's FLD that was fitted to the corrected FLD determined for region B of the center-gated disk. The maximum likelihood method was used for this

Downloaded from jcm.sagepub.com at OAK RIDGE NATIONAL LABORATORY on December 1, 2015

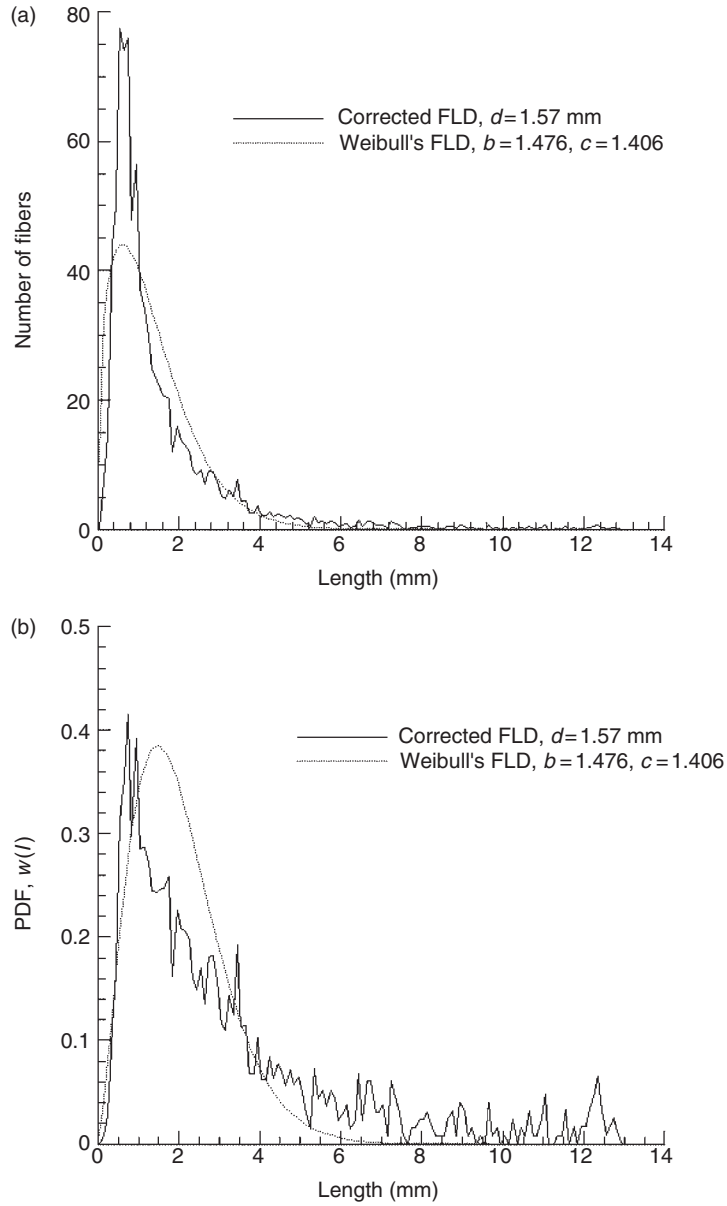

Figure 7. *Corrected FLD in terms of (a) number of fibers vs fiber length and (b) probability density function for weight for the center-gated disk – Weibull's distribution used to fit the corrected FLD data.*

fitting in order to identify the shape parameters b and c. The peak of the experimental distribution is very sharp in the short-fiber range (<1 mm). The parameters b and c identified are 1.476 and 1.406, respectively. Figure 7(b) presents the weight distribution resulting from the Weibull's distribution. The same figure also presents the corrected weight distribution. The results for the ISO-plaque are given in Figure 8(a) and (b). Weibull's parameters identified for this specimen are: $b = 1.143$ and $c = 1.313$.

Downloaded from jcm.sagepub.com at OAK RIDGE NATIONAL LABORATORY on December 1, 2015

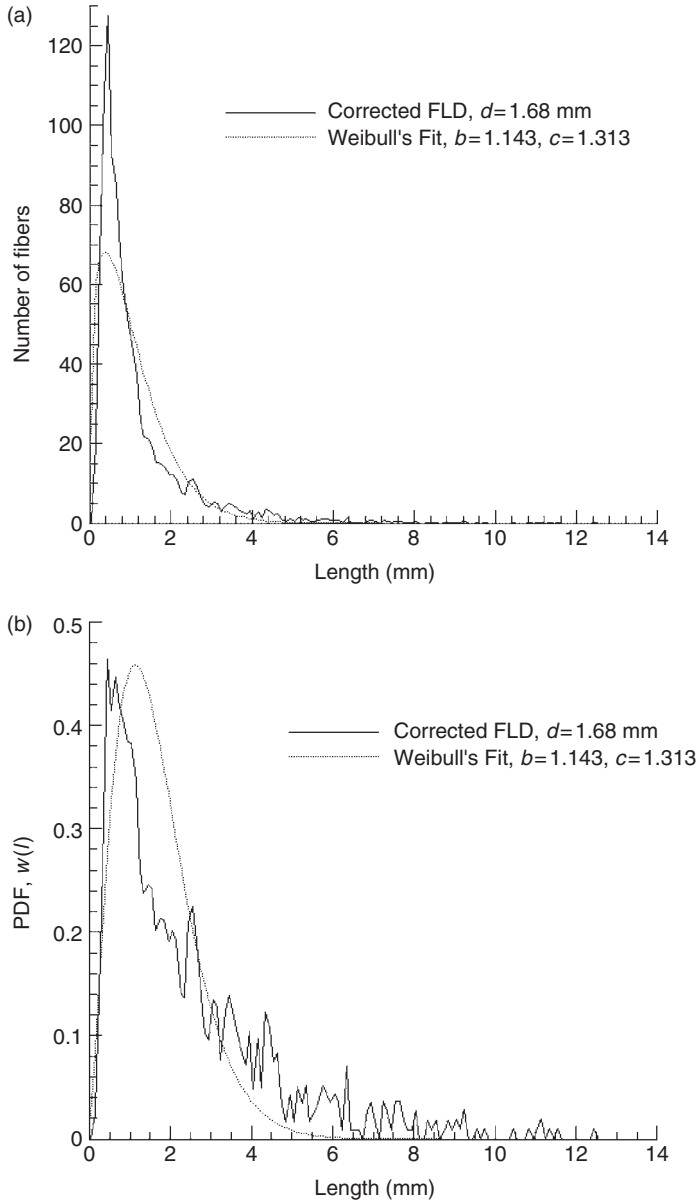

Figure 8. *Corrected FLD in terms of (a) number of fibers vs fiber length and (b) probability density function for weight for the ISO-plaque – Weibull's distribution used to fit the corrected FLD data.*

Figures 7 and 8 show that the two-parameter Weibull's distribution can only fairly represent the distribution in terms of number of fibers versus fiber length in an average manner, and it cannot capture the details of the experimental distribution. However, Weibull's representation for weight of fibers is very good. Table 1 presents the number- and weight-average lengths for both specimens. The average lengths that were obtained from Weibull's distribution fits are very close to the values determined from the

Downloaded from jcm.sagepub.com at OAK RIDGE NATIONAL LABORATORY on December 1, 2015

Table 1. Number-average and weight-average lengths determined from the distributions given in Figures 6 and 7.

	$\bar{L}_n$ (mm)	$\bar{L}_n^{weib}$ (mm)	$\bar{L}_w$ (mm)	$\bar{L}_n^{weib}$ (mm)
ISO-plaque	1.04	1.05	1.83	1.71
Center-gated disk	1.33	1.34	2.18	2.28

actual FLDs. This important feature shows that Weibull's distribution can be used to efficiently represent the FLDs. The computation of elastic properties shows that Weibull's FLD for weight of fibers leads to predicted values of the elastic properties that are very close to the predictions using the corrected experimental FLD.

FOD Data and Differences between Model Predictions and Measurements

The ORIENT code was used to predict fiber orientation in the studied LFT specimens. ORIENT assumes symmetry about the mid-plane in the thickness direction, and this is reflected in the orientation predictions: the predicted values of A_{11}, A_{22}, and A_{33} are all symmetric about $z=0$, while A_{31} is anti-symmetric about $z=0$. The finite difference mesh used in ORIENT consisted of 21 nodes in the thickness direction and 121 nodes in the flow-direction. The parameters SRF and C_I identified for both specimens are 30 and 0.03, respectively. Figure 9(a) and (b) present the orientation predictions for region B of the center-gated disk while Figure 10(a) and (b) show the results for region B of the ISO-plaque. These figures also illustrate the orientation components that were experimentally determined using the Leeds system. There is a reasonably good correlation of results for A_{11}, however, A_{22} is under-predicted, and as a consequence, A_{33} is over-predicted since $A_{11}+A_{22}+A_{33}=1$. A_{31} is poorly fit for both specimens. The orientation distributions in both specimens reveal a skin/shell/core structure through the specimen thickness. This feature has also been observed in short-fiber injection molded materials. The fibers in the skin and shell layers are more aligned in the flow direction characterized by high values of A_{11} and low values of A_{22} while the fiber orientation is rather in the cross-flow direction with high values of A_{22} and low values of A_{11} in the core. The through-thickness-direction A_{33} and A_{31} components are small since long fibers practically remain parallel to the 1–2 plane. The next section will determine the effects of fiber length and orientation distributions on the composite elastic properties.

Elastic Moduli: Predictions versus Experiments

The elastic modulus of glass and polypropylene used in the computation are 73 and 1.5 GPa, respectively. The Poisson's ratios are 0.25 for glass fibers and 0.4 for polypropylene. The fiber length and orientation distributions given in Figures 6, 7 and 9 were used in the computation. The results for the center-gated disk are illustrated for the moduli E_{11}, E_{22}, and E_{33} in Figure 11(a), (b) and (c), respectively. These figures also present the results obtained using Weibull's FLD for weight of fibers given in Figure 6. As Weibull's FLD for weight captures the actual FLD very well, the variations of moduli resulting from the use of this Weibull's distribution are indistinguishable from the results

Downloaded from jcm.sagepub.com at OAK RIDGE NATIONAL LABORATORY on December 1, 2015

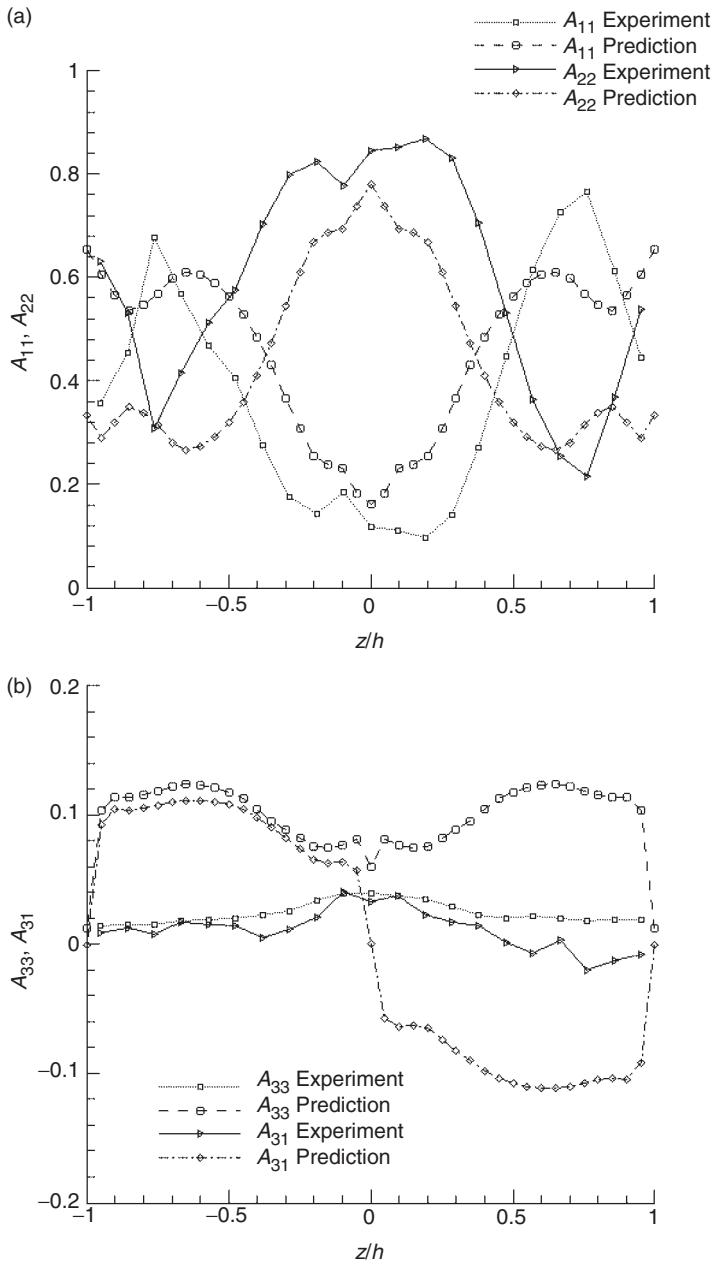

Figure 9. *Predicted and measured second-order orientation components for the center-gated disk: (a) A_{11} and A_{22}, (b) A_{33} and A_{31}.*

using the actual corrected FLD. As the predicted through-thickness variation of A_{11} is closer to the corresponding experimental results this has reflected in the better prediction for the modulus E_{11}. However, the under-prediction for A_{22} has led to under-predicting E_{22}. The moduli predicted for the ISO-plaque are presented in Figure 12(a), (b) and (c).

Downloaded from jcm.sagepub.com at OAK RIDGE NATIONAL LABORATORY on December 1, 2015

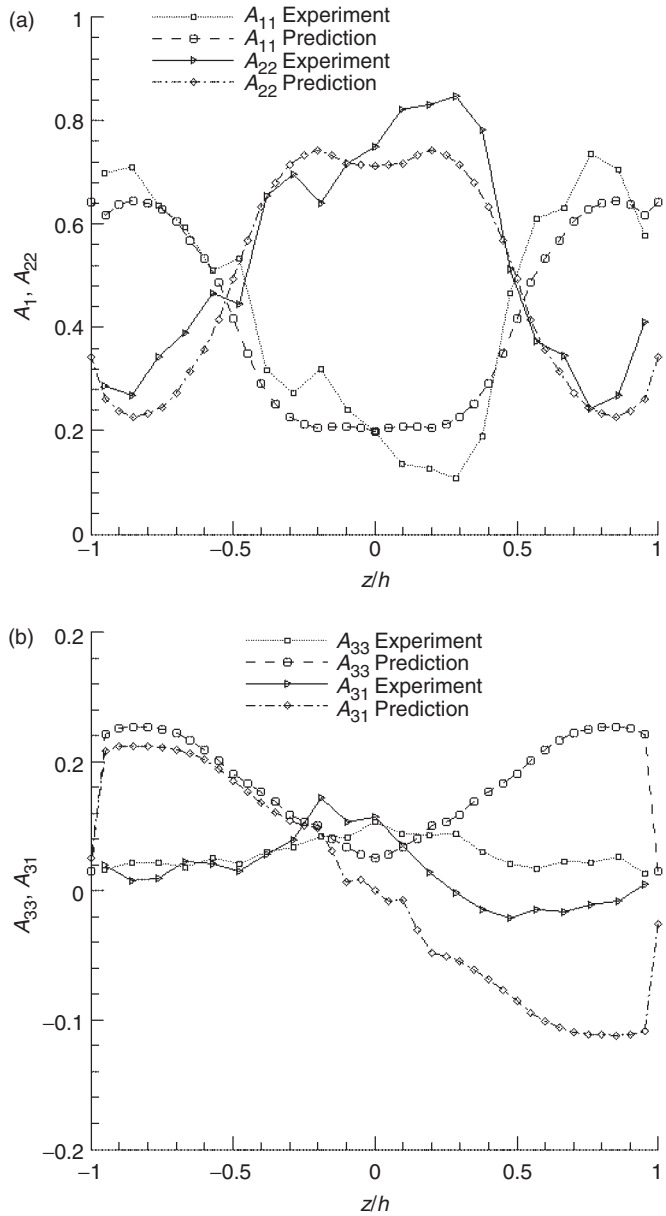

Figure 10. *Predicted and measured second-order orientation components for the ISO-plaque: (a) A_{11} and A_{22}, (b) A_{33} and A_{31}.*

Better correlations between the predicted and experimental results have been found for this specimen.

The overall stiffness of the composite specimen has been determined using the lamination theory and by considering the specimen as being formed by a stacking sequence of composite layers having the same thickness. Tables 2 and 3 present the overall moduli

Downloaded from jcm.sagepub.com at OAK RIDGE NATIONAL LABORATORY on December 1, 2015

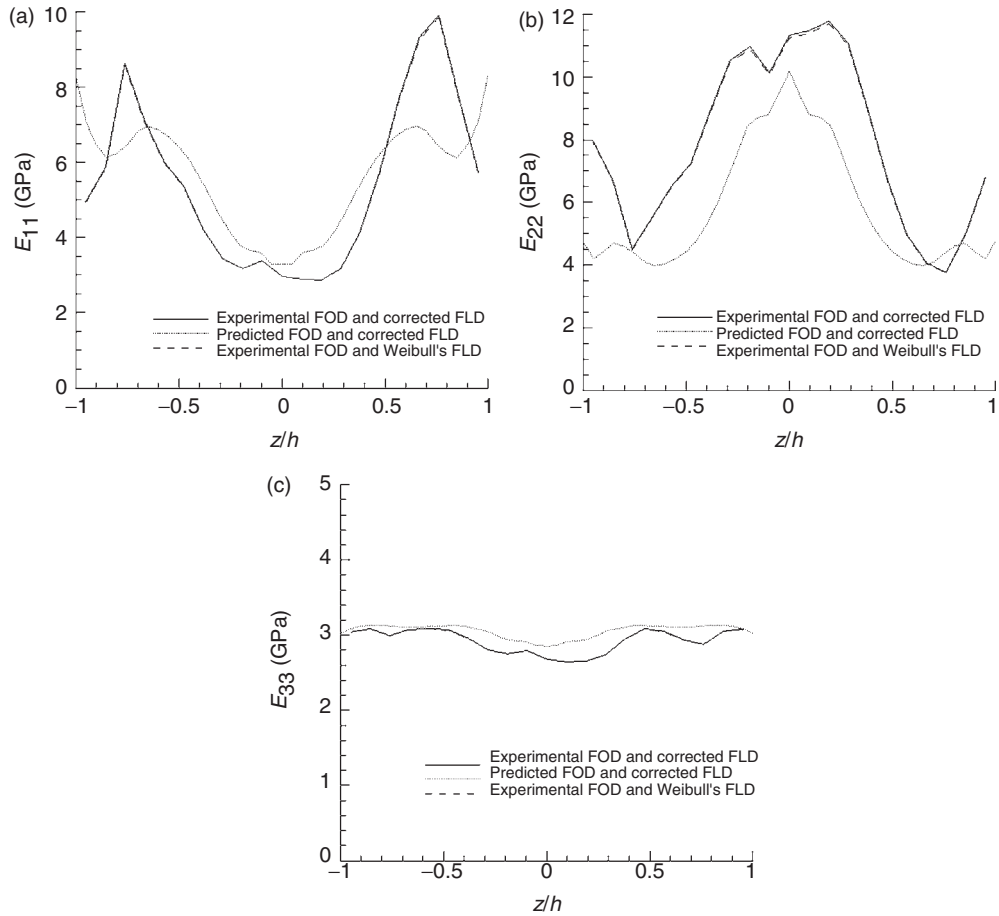

Figure 11. *Predicted through-thickness variation of the elastic moduli (a) E_{11}, (b) E_{22}, and (c) E_{33} for the center-gated disk (the 1-direction is the disk radial direction).*

predicted for the center-gated disk and ISO-plaque. These tables also provide the results computed using Weibull's FLDs and the experimental results for the moduli $\bar{E}_{11}$ and $\bar{E}_{22}$. For each geometry (center-gated disk or ISO-plaque) and for each direction (flow or in-plane cross flow directions), four specimens were tested. The experimental longitudinal and in-plane transverse modulus results were then averaged over four test values for each modulus. Standard deviations (SDV) for the measured values are also given in Tables 2 and 3. There are good correlations between the experimental results and the moduli computed based on the corrected experimental FLDs (Figures 5 and 6) and the experimental FODs. The use of Weibull's FLDs and experimental FODs also provide good predictions. However, the use of the predicted FODs can only provide acceptable predictions for the modulus E_{11}. As previously mentioned, the less accurate prediction of A_{22} has not allowed us to accurately predict the modulus E_{22}. One important conclusion from this study is that the current fiber orientation model can only *qualitatively* capture the fiber orientation distribution in long-fiber thermoplastics. Thus, it cannot provide sufficiently accurate FODs for predictive engineering. Therefore, research is needed to establish a fiber orientation model for LFTs.

Downloaded from jcm.sagepub.com at OAK RIDGE NATIONAL LABORATORY on December 1, 2015

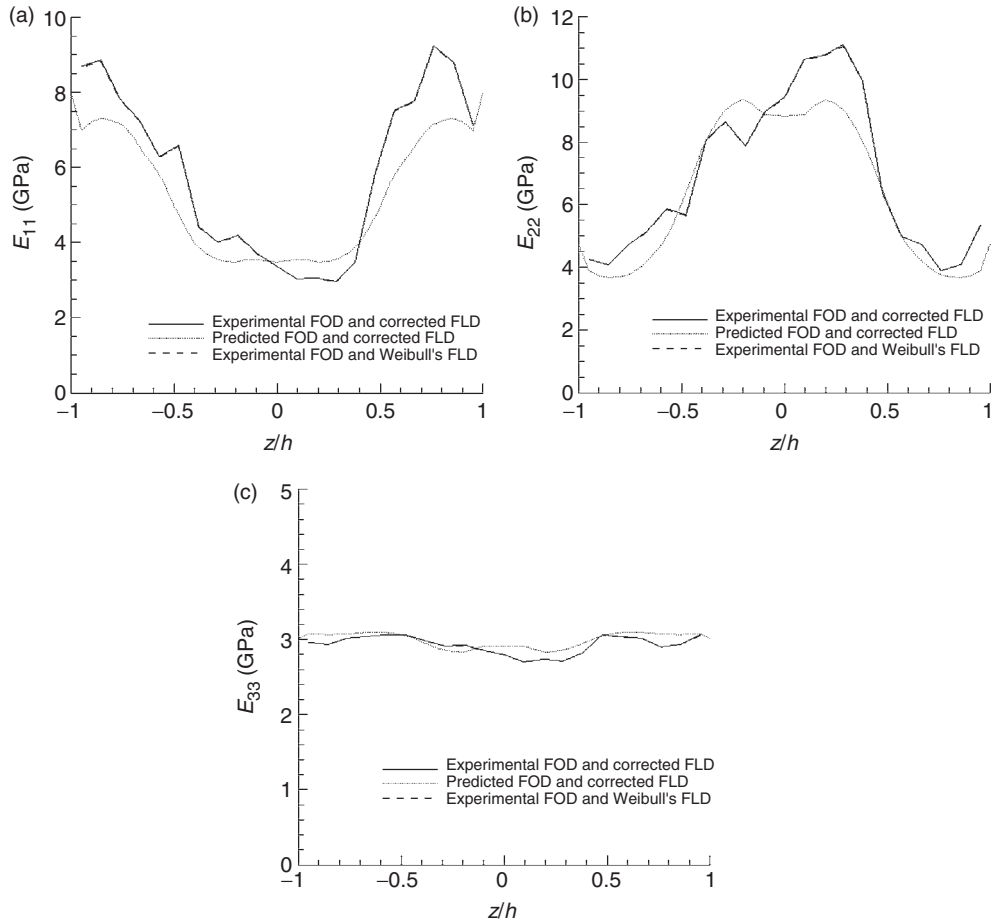

Figure 12. *Predicted through-thickness variation of the elastic moduli (a) E_{11}, (b) E_{22}, and (c) E_{33} for the ISO-plaque (the 1-direction is the plaque longitudinal direction).*

Table 2. Predicted and experimental overall elastic properties for the center-gated disk.

	Predictions (experimental FOD and FLD)	Predictions (predicted FOD and experimental FLD)	Predictions (experimental FOD and Weibull's FLD)	Experiments
$\bar{E}_{11}$ (MPa)	5550	5942	5525	5318 SDV[a] = 122.6
$\bar{E}_{22}$ (MPa)	7907	5826	7863	7521 SDV=16.3
$\bar{E}_{33}$ (MPa)	3068	3141	3063	
$\bar{G}_{12}$ (MPa)	2045	2024	2036	
$\bar{G}_{13}$ (MPa)	940	1311	940	
$\bar{G}_{23}$ (MPa)	1014	1197	1013	

[a]SDV = Standard deviation.

Downloaded from jcm.sagepub.com at OAK RIDGE NATIONAL LABORATORY on December 1, 2015

Table 3. Predicted and experimental overall elastic properties for the ISO-plaque.

	Predictions (experimental FOD and FLD)	Predictions (predicted FOD and experimental FLD)	Predictions (experimental FOD and Weibull's FLD)	Experiments
$\bar{E}_{11}$ (MPa)	6017	5361	6001	6063 SDV = 181.1
$\bar{E}_{22}$ (MPa)	6935	6377	6916	7211 SDV = 479
$\bar{E}_{33}$ (MPa)	3070	3109	3068	
$\bar{G}_{12}$ (MPa)	2046	1916	2041	
$\bar{G}_{13}$ (MPa)	977	1194	977	
$\bar{G}_{23}$ (MPa)	1010	1165	1010	

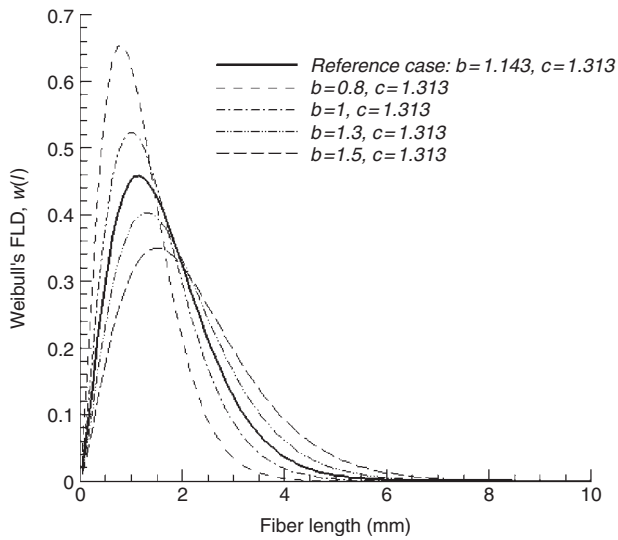

Figure 13. *Weibull's probability density functions for weight of fibers generated by varying Weibull's parameter b around its reference value for the ISO-plaque.*

Parametric Study of Weibull's Parameters and FLD Effects

This section analyzes the effect of a variation of FLD on the elastic properties of the studied ISO-plaque. In view of the difficulty to capture the true FLD through experimental characterization, it is important to know whether some deviations between the measured and true FLDs can have a significant effect on the predicted elastic properties of the composite. To this end, Weibull's distribution previously used to fit the corrected experimental FLD for this specimen is considered first as the reference FLD. The values of the identified shape parameters b and c are then considered as the reference values around which some variations were prescribed to study their effects on the composite elastic properties. Such an analysis provides some insights as to whether the capture of the true FLD is absolutely necessary and whether some deviations of the measured FLD with respect to the true FLD are acceptable.

Figure 13 shows Weibull's FLDs that were obtained by varying the shape parameter b around the reference value of 1.143. The values of b considered are 0.8, 1, 1.3, and 1.5

Downloaded from jcm.sagepub.com at OAK RIDGE NATIONAL LABORATORY on December 1, 2015

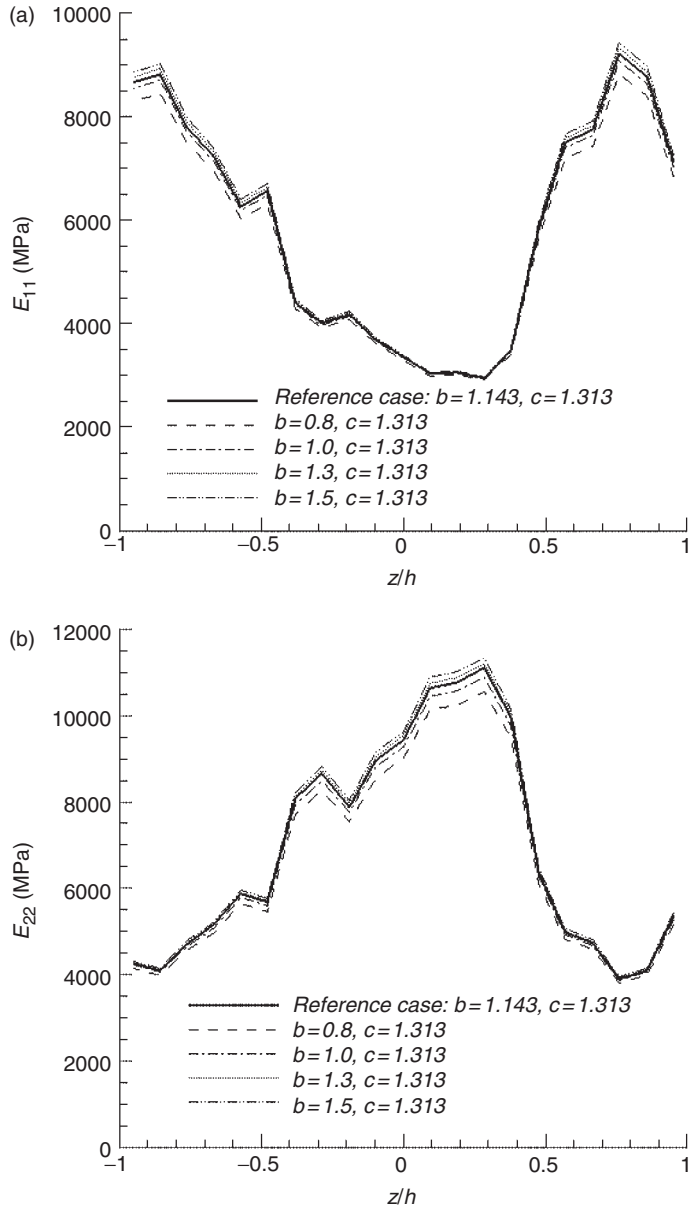

Figure 14. *Predicted through-thickness variation of the elastic moduli (a) E_{11}, and (b) E_{22} for the ISO-plaque as the result of the variation of Weibull's parameter b.*

while the value of parameter c is kept constant ($c = 1.313$). Increasing parameter b widens the distribution towards the long-fiber range and decreases its peak while decreasing b sharpens it and moves its peak towards the short-fiber range. Figure 14 (a) and (b) present the through-thickness variations of the moduli E_{11} and E_{22} resulting from the generated FLD distributions and the experimental fiber orientation distribution (Figure 10). The values of the elastic moduli obtained using the reference FLD are

Downloaded from jcm.sagepub.com at OAK RIDGE NATIONAL LABORATORY on December 1, 2015

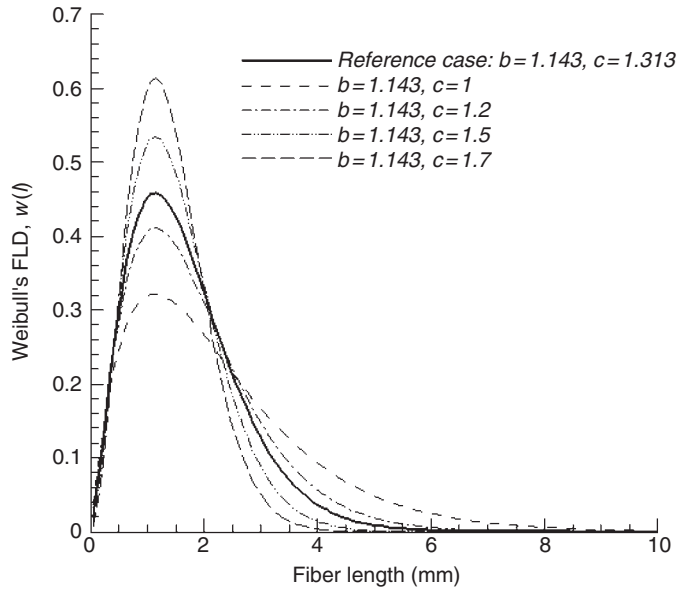

Figure 15. *Weibull's probability density functions for weight of fibers generated by varying Weibull's parameter c around its reference value for the ISO-plaque.*

considered as the reference values. For E_{11}, the maximum deviations with respect to the reference values occur in the skin and shell layers whereas for E_{22}, the highest deviations happen in the core. A significant shift of a FLD with respect to the reference FLD towards the long-fiber range only results in very small increases in the elastic moduli, however, a significant shift of a FLD towards the short-fiber range will induce larger reductions of the moduli. For the values of the shape parameter b considered, the most important reduction in E_{11} happens in the shell layers for $b = 0.8$ while for E_{22} the highest deviation for this value of b is found in the core.

In the second sensitivity analysis, the shape parameter b was kept constant ($b = 1.143$) while different values of parameter c around the reference value were prescribed to generate the corresponding FLDs. The values of c considered are 1, 1.2, 1.5 and 1.7. Figure 15 shows Weibull's FLDs that were obtained based on these prescribed values of b and c. Increasing parameter c sharpens the distribution, increases its peak, and very slightly moves it towards the long-fiber range while decreasing c widens the distribution towards the long-fiber range, decreases the distribution's peak and just very slightly shifts it towards the short-fiber range. Figure 16(a) and (b) show the through-thickness variations of the moduli E_{11} and E_{22} resulting from the generated FLDs and the experimental FOD. With respect to the previous case, a somewhat different conclusion is made for the present case. By examining the FLDs given in Figure 15, it can be seen that the peaks of all the generated FLDs occur around $l = 1.1$ mm, and with increasing value of c from 1 to 1.7, the distribution is sharpened but its peak increases. Initially, increasing c results in an increase of the moduli, but from a certain value of c, the distribution becomes sharp, and this reduces the weight of long fibers, and consequently reduces the moduli. However, Figure 16(a) shows clearly that the effect of varying c is negligible. Tables 4 and 5 present the overall

Downloaded from jcm.sagepub.com at OAK RIDGE NATIONAL LABORATORY on December 1, 2015

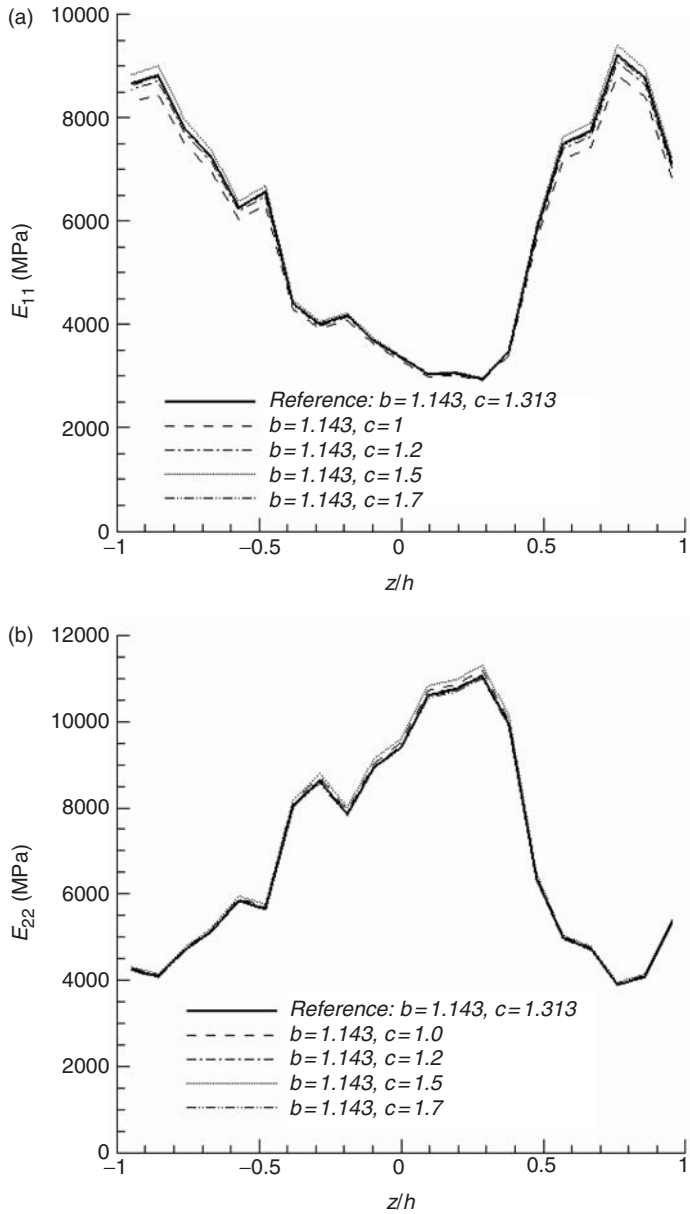

Figure 16. *Predicted through-thickness variation of the elastic moduli (a) E_{11}, and (b) E_{22} for the ISO-plaque as the result of the variation of Weibull's parameter c.*

moduli $\bar{E}_{11}$ and $\bar{E}_{22}$ obtained by varying the shape parameters b and c around their reference values. Since all the percentages of deviation with respect to the reference cases are less than 5%, the sensitivity analysis has shown that some deviations of the FLD with respect to the actual FLD do not significantly affect the predicted elastic properties.

Downloaded from jcm.sagepub.com at OAK RIDGE NATIONAL LABORATORY on December 1, 2015

Table 4. Predictions of the overall moduli $\bar{E}_{11}$ and $\bar{E}_{22}$ using the FLDs generated in Figure 12 (variation of parameter b) and the experimental fiber orientation for the ISO-plaque.

	$b = 0.8$	$b = 1$	$b = 1.143$ (reference)	$b = 1.3$	$b = 1.5$	Experiment
$\bar{E}_{11}$	5788	5930	6001	6061	6118	6063
$\bar{E}_{22}$	6648	6826	6916	6991	7062	7211

Table 5. Predictions of the overall moduli $\bar{E}_{11}$ and $\bar{E}_{22}$ using the FLDs generated in Figure 14 (variation of parameter c) and the experimental fiber orientation for the ISO-plaque.

	$c = 1$	$c = 1.2$	$c = 1.313$ (reference)	$c = 1.5$	$c = 1.7$	Experiment
$\bar{E}_{11}$	6051	6015	6001	6102	5978	6063
$\bar{E}_{22}$	6978	6933	6916	7041	6886	7211

CONCLUSIONS

This article has developed a rigorous methodology to determine the elastic properties of long-fiber injection-molded thermoplastics. This methodology combines process modeling and micromechanical modeling based on the EMT model with experimental characterization of fiber length and orientation distributions. It has been shown that it is indispensable to obtain an accurate fiber orientation distribution and a realistic fiber length distribution in order to accurately predict the composite properties. The current fiber orientation model cannot predict the fiber orientation in LFT samples to a level of accuracy needed for accurate property prediction. Therefore, research is really needed to develop a fiber orientation model for LFTs. The correction for the raw FLD data is necessary to obtain a more realistic fiber length distribution. The developed methodology has been validated via experimental verification of the longitudinal and in-plane transverse moduli determined for long glass fiber injection-molded polypropylene specimens. The use of the corrected FLD for weight of fiber lengths and the experimental FOD has allowed good predictions of the elastic properties for the studied glass/PP specimens. Weibull's FLD can very well capture the actual FLD for weight of fibers, thus the use of the Weibull's distribution for weight has led to practically the same results as those obtained using the actual FLD.

An important conclusion from the sensitivity analysis of FLD variation is that in long-fiber thermoplastics, if the remaining average lengths still allow sufficiently high values of the average fiber aspect ratios, the elastic properties start reaching the limits for continuous fibers. Therefore, some shifts of the FLD towards long-fiber range will not significantly affect the predicted properties. On the other hand, the measurement error that displaces the FLD towards the short-fiber range does have a greater effect.

ACKNOWLEDGMENTS

This work has been funded by the U.S. Department of Energy's Office of FreedomCAR and Vehicle Technologies. The support by Dr. Joseph Carpenter Jr, Technology Area Development Manager, is gratefully acknowledged. We would like to thank

Downloaded from jcm.sagepub.com at OAK RIDGE NATIONAL LABORATORY on December 1, 2015

Moldflow, Inc. for the rheological and physical data measurement for the glass/polypropylene material studied in this article.

REFERENCES

1. Truckenmüller, F. and Fritz, H.-G. (1991). Injection Molding of Long Fiber-Reinforced Thermoplastics: A Comparison of Extruded And Pultruded Materials With Direct Addition of Roving Strands, *Polymer Engineering and Science*, **31**: 1316–1329.
2. Silverman, E.M. (1987). Effect of Glass Fiber Length on the Creep and Impact Resistance of Reinforced Thermoplastics, *Polymer Composites*, **8**: 8–15.
3. Henning, F., Ernst, H., Brussel, R., Geiger, O. and Krause, W. (2005). LFTs for Automotive Applications, *Reinforced Plastics*, **49**: 24–33.
4. Hine, P.J., Davidson, N., Duckett, R.A., Clarke, A.R. and Ward, I.M. (1996). Hydrostatically Extruded Glass-Fiber-reinforced Polyoxymethylene. I: The Development of Fiber and Matrix Orientation, *Polymer Composites*, **17**: 720–729.
5. Kunc, V., Frame, B.J., Nguyen, B.N., Phelps, J.H. and Tucker III, C.L. (2008). Fiber Length and Orientation in Long-Fiber Injection-molded Thermoplastics – Part II: Experimental Characterization of Microstructure. *In preparation*.
6. Gupta, V.B., Mittal, R.K., Sharma, P.K., Mennig, G. and Wolters, J. (1989). Some Studies on Glass Fiber-Reinforced Polypropylene. Part II: Mechanical Properties and Their Dependence on Fiber Length, Interfacial Adhesion, and Fiber Dispersion, *Polymer Composites*, **10**: 16–27.
7. Vu-Khanh, T., Denault, J., Habib, P. and Low, A. (1991). The Effects of Injection Molding on the Mechanical Behavior of Long-Fiber Reinforced PBT/PET blends, *Composites Science and Technology*, **40**: 423–435.
8. Advani, S. and Tucker III, C.L. (1987). The Use of Tensors to Describe and Predict Fiber Orientation in Short-Fiber Composites, *Journal of Rheology*, **31**: 751–784.
9. Camacho, C., Tucker III, C.L., Yalvac, S. and McGee, R.L. (1990). Stiffness and Thermal Expansion Predictions for Hybrid Short-Fiber Composites, *Polymer Composites*, **11**: 229–239.
10. Eshelby, J.D. (1957). The Determination of the Elastic Field of an Ellipsoidal Inclusion and Related Problems, *Proceedings of the Royal Society London*, **A241**: 376–396.
11. Mori, T. and Tanaka, K. (1973). Average Stress in Matrix and Average Elastic Energy of Materials With Misfitting Inclusions, *Acta Metallurgica*, **21**: 571–574.
12. Benveniste, Y. (1987). A New Approach to the Application of Mori-Tanaka's Theory in Composite Materials, *Mechanics of Materials*, **6**: 147–157.
13. Tucker III, C.L. and Liang, E. (1999). Stiffness Predictions for Unidirectional short-fiber Composites: Review and Evaluation, *Composites Science and Technology*, **59**: 655–671.
14. Hine, P.J., Lusti, H.R. and Gusev, A.A. (2002). Numerical Simulation of the Effects of Volume Fraction, Aspect Ratio and Fiber Length Distribution on the Elastic and Thermoelastic Properties of Short Fiber Composites, *Composites Science and Technology*, **62**: 1445–1453.
15. Tandon, G.P. and Weng, G.J. (1984). The Effect of Aspect Ratio of Inclusions on the Elastic Properties of Unidirectionally Aligned Composites, *Polymer Composites*, **5**: 327–333.
16. Hine, P.J., Lusti, H.R. and Gusev, A.A. (2004). On the Possibility of Reduced Variable Predictions for the Thermoelastic Properties of Short Fiber Composites, *Composites Science and Technology*, **64**: 1081–1088.
17. Taya, M. and Mura, T. (1981). On stiffness and Strength of an Aligned Short-Fiber Reinforced Composite Containing Fiber-End Cracks Under Uniaxial Applied Stress, *Journal of Applied Mechanics*, **48**: 361–367.
18. Chen, C.-H. and Cheng, C.-H. (1996). Effective Elastic Moduli of Misoriented Short-Fiber Composites, *International Journal of Solids and Structures*, **33**: 2519–2539.
19. Kunc, V., Frame, B.J., Nguyen, B.N., Tucker III, C.L. and Velez-Garcia, G. (2007). Fiber Length Distribution Measurement for Long Glass and Carbon Fiber Reinforced Injection

Downloaded from jcm.sagepub.com at OAK RIDGE NATIONAL LABORATORY on December 1, 2015

Molded Thermoplastics. In: *Proceedings of the 7th Annual SPE Automotive Composites Conference and Exposition*. Society of Plastic Engineers, Troy, Michigan.

20. Chin, W.-K., Liu, H.-T. and Lee, Y.-D. (1988). Effect of Fiber Length and Orientation Distribution on the Elastic Modulus of Short Fiber Reinforced Thermoplastics, *Polymer Composites*, **9**: 27–35.
21. Iuculano, G., Nielsen, L., Zanobini, A. and Pellegrini, G. (2007). The Principle of Maximum Entropy Applied in The Evaluation of The Measurement Uncertainty, *IEEE Transactions on Instrumentation and Measurement*, **56**(3): 717–722.
22. ASTM International (2005). Standard Practice for Reporting Uniaxial Strength Data and Estimating Weibull Distribution Parameters for Advanced Ceramics. C1239–06.
23. Cintra Jr, J.S. and Tucker III, C.L. (1995). Orthotropic Closure Approximations for Flow-Induced Fiber Orientation, *Journal of Rheology*, **39**: 1095–1122.
24. Wetzel, E.D. (1999). Modeling Flow-induced Microstructure in Inhomogeneous Liquid-liquid Mixtures. Ph.D. thesis, University of Illinois at Urbana-Champaign, Urbana, IL.
25. Bay, R.S. and Tucker III, C.L. (1992). Fiber Orientation in Simple Injection Moldings. Part I: Theory and Numerical Methods, *Polymer Composites*, **13**: 317–331.
26. Lee, C.C., Folgar, F. and Tucker III, C.L. (1984). Simulation of Compression Molding for Fiber Reinforced Thermosetting Polymers, *Journal of Engineering Industry*, **106**: 114–125.
27. Tucker III, C.L., Wang, J. and O'Gara, J.F. (2007). Method and article of manufacture for determining a rate of change of orientation of a plurality of fibers disposed in a fluid. U.S. Patent No. 7,266,469. See also Wang, J., O'Gara, J.F. and Tucker III, C.L. (2007). An Objective Model for Slow Orientation Kinetics in Concentrated Fiber Suspensions: Theory and Rheological Evidence. *Journal of Rheology* (submitted).
28. Folgar, F. and Tucker III, C.L. (1984). Orientation Behavior of Fibers in Concentrated Suspensions, *Journal of Reinforced Plastic Composites*, **3**: 98–119.
29. Toll, S. and Anderson, P.-O. (1993). Microstructure of Long- and Short-Fiber Reinforced Injection Molded Polyamide. *Polymer Composites*, **14**(2): 116–125.
30. Bapanapalli, S.K. and Nguyen, B.N. (2007). Prediction of Elastic Properties for Curved fiber Composites, *Polymer Composites* (in press).

Downloaded from jcm.sagepub.com at OAK RIDGE NATIONAL LABORATORY on December 1, 2015